J Mater Sci: Mater Med (2010) 21:2561–2568
DOI 10.1007/s10856-010-4117-2

Bone-like nanocomposites based on self-assembled protein-based matrices with Ca^{2+} capturing capability

Lin Sang · Jie Huang · Dongmei Luo · Zhenhua Chen · Xudong Li

Received: 27 November 2009 / Accepted: 11 June 2010 / Published online: 27 June 2010

Abstract In the present work, bone-like nanocomposites have been successfully synthesized based on the mineralization of self-assembled protein-based microgels. Such mircogels were achieved by the in vitro reconstitution of collagen monomeric solutions in the presence of alginate in a microemulsion system. Microstructural observations revealed that the collagen-alginate composite beads possessed a nanofibrous three dimensional (3D) interconnected porous microstructure. The obtained microgels were pre-incubated in calcium-containing solution to capture Ca^{2+} ions, and subsequently immersed in phosphate-containing solution to initiate the formation of hydroxyapatite (HA) by an alternative incubating procedure. It was observed that a substantial amount of bone-like apatite nanocrystals were orderly and homogeneously deposited throughout the porous fibrillar networks. Herein, the collagen-alginate composite microgels served as a mineralization template for the synthesis of HA-polymer nanocomposites, which could be ideal vehicles potentially for cell carriers, bone repair and proteins and drugs delivery in tissue regeneration.

1 Introduction

The inorganic/organic biocomposites consisting of hydroxyapatite (HA) and natural polymers such as proteins (i.e. collagen or gelatin), and polysaccharides [1, 2] have been extensively investigated in the fields of tissue engineering, implants, drug delivery systems, and protein chromatography [3–5]. The biomimetic combination of biocompatible polymers and HA is believed to possess synergistic effects of well-organized structure and topography, biologically active interface, improved mechanical properties and controlled release behaviors. The mostly claimed underlying mechanism for the biomimetic synthesis of HA-polymer nanocomposites suggested that the mineralization occurs involving the deposition of inorganic phase on the macromolecular framework, which is believed to serve as a template to mediate the nucleation and growth of apatite as well as to regulate the size, morphology, and orientation of mineral crystals [1, 3, 5].

It is worthy to note that the anionic groups of biopolymers exposed in the reactive solution are capable of enriching the Ca^{2+} ions, leading to a local supersaturation and then inducing the nucleation of HA. Previous studies also demonstrated that the apatite nucleation was enhanced and accelerated in the conditions that the carboxyl/phosphate group-containing polymers have been pre-combined with calcium ions [6–9]. Both the density of the charged groups and the intensity of the interactions between polymeric matrix and the inorganic groups would influence the formation of HA, meanwhile the accessibility of these functional groups on the framework is also of importance in this biomimetic mineralization process.

Type I collagen is the major structural protein of bone and also a rational candidate biomaterial for soft tissue repair and bone tissue reconstruction. Extensive investigations have been undertaken for the study of collagen as the biomimetic synthesis template to develop biomineralized tissue materials [10, 11]. A self-assembled collagen

L. Sang · D. Luo · Z. Chen · X. Li (✉)
National Engineering Research Center for Biomaterials, Sichuan University, Chengdu 610064, People's Republic of China
e-mail: xli20004@yahoo.com

J. Huang
Department of Mechanical Engineering, University College London, Torrington Place, London WC1E 7JE, UK

matrix with the nativelike fibrils could be obtained on the basis of in vitro reconstitution of collagen monomeric solutions into collagen fibrils at proper conditions. The 3D network fibrillar architecture analogous to the natural extracellular matrix enables collagen as a template for mineral deposition [1]. Recent studies have focused on the surface functionalization of collagen such as the phosphorylation and carboxylation of surface modification [9, 12] to develop an anionic collagen matrix to induce the nucleation of apatite. Such a strategy requires the selection of targeted groups on collagen and possibly changes the behavior of microfibrillar assembly. However, only in a few cases has it been introduced the polysaccharides with charged groups into the collagen matrix instead of applying complicated surface modification [13]. According to the strategy, the designed composite materials are endowed with charged functional groups which may become quite effective in the biomimetic mineralization process.

Alginate is a linear anionic polysaccharide copolymer consisting of (1 → 4) linked β-D-mannuronate (M) and its C-5 epimer α-L-guluronate (G) units in varying proportions, and its wide applications for the tissue regeneration of cartilage [14], skin [15], bone [1] and liver [16] have been demonstrated the excellent biocompatibility. The salient features of alginate include the strong ionic interactions of the carboxylic groups located on the polymeric backbone with multivalent cations (i.e., Ca^{2+}) and with other polyelectrolytes [17, 18]. In particular, alginate is capable of attracting and capturing calcium ions, acting as nucleation agents to encourage apatite nucleation. Therefore, it is expected that the introduction of alginate into collagen matrix could afford plentiful carboxyl groups and improve the calcium-binding efficiency in the performance of biomimetic mineralization.

In the present work, self-assembled collagen-alginate composite beads with the Ca^{2+}-captured capacity were fabricated in order to realize the biomimetic synthesis of HA/polymer nanocomposites. These composite beads were fibrillar matrices obtained by the in vitro reconstitution of collagen monomeric solutions in the presence of alginate through a microemulsion system. Among a certain number of techniques now available to synthesize polymer-HA hybrid composites, the biomimetic process by soaking in a simulated body fluid would require an incubation period up to one week for securing a homogenous biomimetic apatite layer [8, 9, 19] whereas the alternative soaking procedure could form a homogeneous biomimetic apatite layer in a much shorter time [7, 20, 21]. Hence, the present study developed the self-assembled collagen-alginate composite beads with Ca^{2+} capacity as a potential template to biomimetic mineralization via the alternative incubating procedure.

2 Materials and methods

2.1 Materials

Type I collagen was extracted in our laboratory from calf skin by pepsin digestion. Alginate (2 wt%, 30–60 cps at 20°C) was purchased from Sigma. Olive oil and glutaraldehyde were purchased from Kelong Chemical Agent Factory, Chengdu, China. All the other reagents were analytical grade and used without further purification.

2.2 Preparation of collagen-alginate (Coll-Alg) composite beads

The collagen-alginate (Coll-Alg) beads with a diameter of 500–1500 μm were prepared by using a water-in-oil emulsion system as described in the reference 22. Briefly, acidic collagen solution was neutralized to a pH of 7.4 by 2 M sodium hydroxide at 4°C. 2% (w/v) alginate aqueous solution was added to neutral collagen solution in a ratio of collagen/alginate = 4:1 (w/w), and then homogenized with magnetic stirring for 2 h at 4°C. Neutralized collagen solution was prepared as a control.

An aliquot of 3 ml olive oil was pre-warmed at 37°C. 1 ml Coll-Alg mixed solution prepared above was added to olive oil slowly. The mixture was emulsified while being slowly stirred at 60 rpm. After stirring at 37°C water bath for 2 h, gluteraldehyde was added to crosslink the aqueous phase of Coll-Alg mixture (final concentration of 2.5% (v/v)) and kept stirring for another 1 h. The emulsions of Coll-Alg microdroplets became white and solid, indicating that the gelation of Coll-Alg was underway. The emulsification was left overnight without stirring at 37°C to allow the thorough reconstitution of collagen in the presence of alginate. Solid Coll-Alg composite beads were collected after washing with petroleum ether, ethanol for 3 times to ensure no residual gluteraldehyde and olive oil. Pure collagen beads were also prepared as the control to reveal the effect of alginate on the nanofibrous network under similar conditions.

2.3 Deposition of hydroxyapatite (HA) in the Coll-Alg composite beads

The deposition of calcium phosphate in Coll-Alg microgels were carried out according to the alternative soaking procedure. HA was formed in Coll-Alg fibrillar beads by performing alternative incubations in calcium- and phosphate-containing solutions. In brief, the Coll-Alg beads were firstly incubated in 0.5 M $CaCl_2$ solutions at 25°C for 24 h to absorb and capture calcium ions. Then the beads were washed with double distilled water for three times to remove any loosely adsorbed Ca^{2+} ions. Finally, the

Ca-captured beads were transferred into 0.3 M Na_2HPO_4 solution for 10 h to initiate inorganic phase deposition. The above HA formation steps were repeated three cycles to obtain stable Coll-Alg-HA nanocomposite beads. After the mineralization process, the nanocomposite beads were thoroughly washed with double distilled water and then freeze-dried for 36 h to obtain the dried nanocomposite beads.

2.4 Characterization

The morphology and the microstructure of lyophilized Coll-Alg and Coll-Alg-HA nanocomposite beads were observed on a field emission scanning electron microscope (FE-SEM, Hitachi, S-4800N). All samples were sputter coated with a thin layer of gold to avoid electrical charging, and observed at an accelerating voltage of 5 kV. Compositional information was assessed by energy dispersive X-ray analysis (EDX) to scan a well-defined area of the Coll-Alg-HA sample. Optical photos of Coll-Alg and Coll-Alg-HA beads were taken through a microscope eyepiece with micrometric scale (Olympus IX 71) or taken together with a metric scale through a digital camera. The diameters of the imaged beads were then measured using the projected scale as reference. The mean diameter of the beads was calculated from a sample number of 200 beads ($n = 200$).

Dried powders of Coll-Alg and Coll-Alg-HA samples were mixed with KBr and pressed to a plate for Fourier transform infrared spectroscopy measurements (FT-IR, Perkin-Elmer Spectrum One B system). The spectra were collected in the range of 4,000–400 cm^{-1} at a 4 cm^{-1} resolution and 20 scan accumulations.

The crystalline phase of calcium phosphate nanocrystals deposited on the Coll-Alg fibrillar networks was determined on a Y-2000 automated X-ray diffractometer system (XRD, Cu Kα radiation, $\lambda = 0.15406$ nm), operating at 30 kV, 30 mA. The relative intensities were recorded within the range of 10–60° (2θ) at a scanning speed of 2°/min. The phase identification was performed with a reference to the JCPDS data cards.

To assess the deposition efficiency, thermal analysis (TGA, NETZSCH STA 449C) were conducted with a scanning temperature from 35 up to 800°C at a controller rate of 10°C/min in a nitrogen atmosphere with an empty aluminum pan as a reference. The dried samples were weighed about 5 mg, and placed in an aluminum pan ($n = 3$).

3 Results and discussion

The synthesis of Coll-Alg-HA nanocomposites was schematically depicted in Fig. 1. Briefly, the nanocomposite beads were obtained via a two-step process involving: (i) the formation of collagen-alginate composite beads through the self-assembly of collagen fibrils in the presence of alginate in a water-in-oil emulsion and then crosslinked with glutaraldehyde; and (ii) the mineralization of Coll-Alg microgels via the alternative soaking process in calcium- and phosphate-containing solutions. The obtained Coll-Alg beads possessed a three-dimensional (3D) interconnected porous structure and had good elasticity. When the Coll-Alg beads were pre-incubated in the calcium-containing solution, the open pores permitted the ease infiltration of calcium ions throughout the Coll-Alg fibrillar networks [23]. Owing to the strong associations of calcium ions with the active radicals of Coll-Alg matrices including anionic functional groups of alginate, calcium ions were effectively

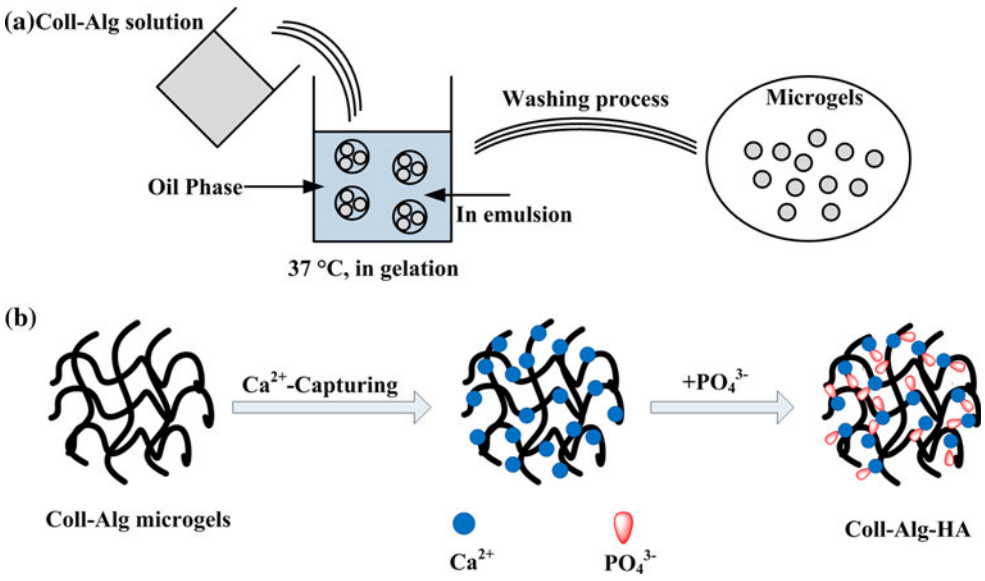

Fig. 1 Schematic representation of the Ca-capturing strategy for the synthesis of collagen-alginate-hydroxyapatite nancomposite beads. **a** Assembly of collagen-alginate solution into fibrillar microgels in a microemulsion system, **b** capturing calcium ions by incubation of microgels in Ca-containing solution and then HA synthesis in phosphate-containing solution

immobilized onto the surface of the Coll-Alg fibrillar matrices during the pre-incubation process. When the phosphate groups were introduced, they were interacted with calcium ions captured on the organic matrices, and thereby initiated the deposition of HA [1, 3].

3.1 Morphological assessment of Coll-Alg matrices for deposition

The effect of alginate on the nanofibrous networks of Coll-Alg beads was examined in comparison with the pure collagen beads. SEM images of lyophilized collagen and Coll-Alg beads are presented in Fig. 2. Pure collagen beads show an appreciable shrinkage after lyophilization, and possess a relatively tight structure with a smooth surface (Fig. 2a). At magnified images (Fig. 2b and 2c), dense and interlaced collagen nanofibers with the mean diameter smaller than 150 nm are observed on the smooth surface (Fig. 2c). In contrast, Coll-Alg beads well preserved their shape and exhibited a well-organized 3D open porous architecture (Fig. 2d). Their pores were constructed by fibrous objects (Fig. 2e, f). Obviously, the introduction of alginate into collagen in the present study enhanced the structural integrity of microgels.

Accordingly, the Coll-Alg fibrillar beads were selected to prepare Coll-Alg-HA nanocomposite beads via an alternative soaking process. After the mineralization process, the mineralized Coll-Alg microgels and their lyophilized products were examined with a light microscope and a digital camera, respectively (Fig. 3). The optical image of the mineralized Coll-Alg microgels revealed the homogeneity of the inorganic phase deposition, suggesting that the mineralization process occurred throughout the whole microgels instead of merely coating onto the outer surface (Fig. 3a). After lyophilizing the mineralized Coll-Alg microgels, spherical nanocomposite beads were obtained (Fig. 3b). The mean diameter of Coll-Alg-HA nanocomposite beads was in a range of 1–2 mm.

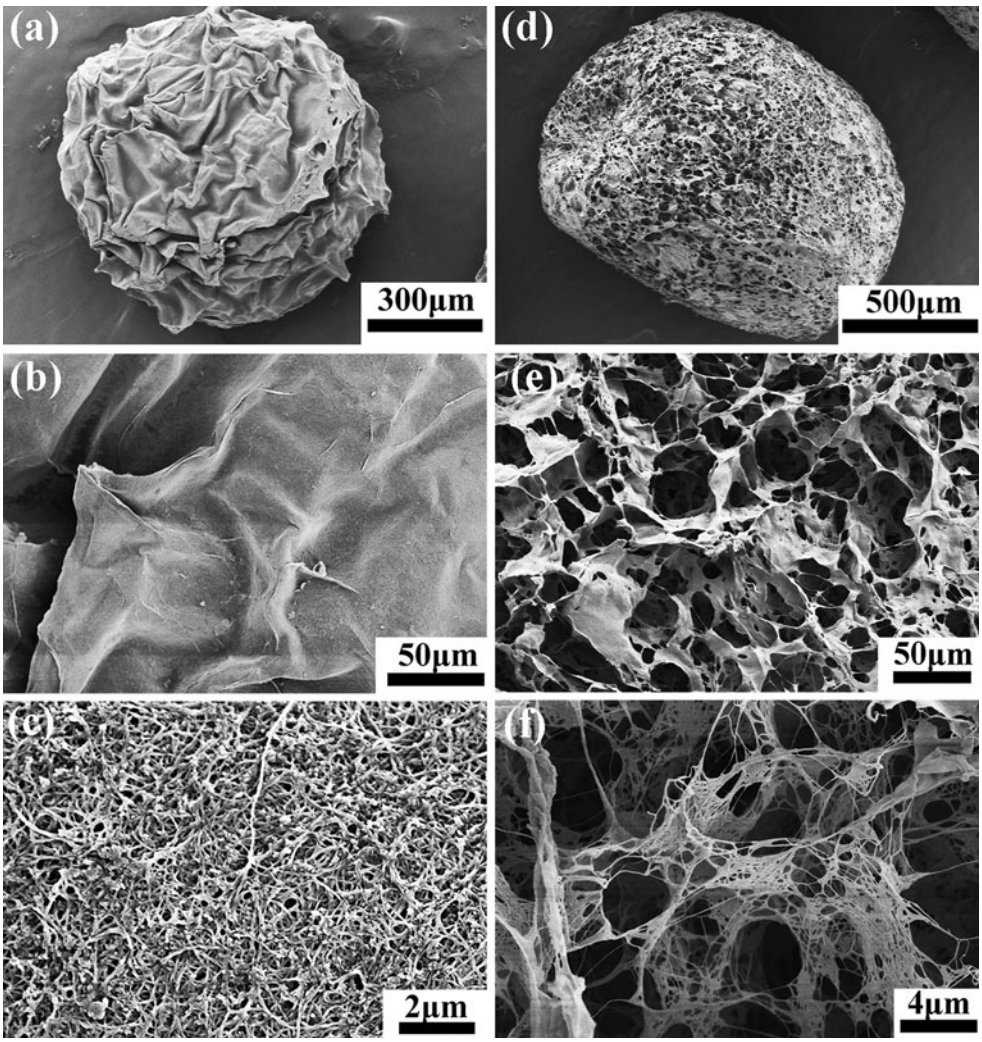

Fig. 2 Comparative SEM images of (**a–c**) lyophilized pure collagen matrices and (**d–f**) lyophilized Coll-Alg composite matrices

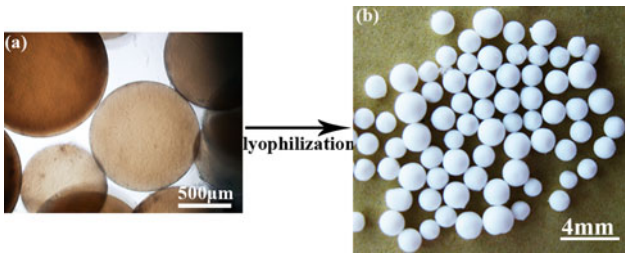

Fig. 3 **a** Optical image of mineralized Coll-Alg microgels and **b** photo of lyophilized Coll-Alg-HA beads

The cross sectional SEM images of the Coll-Alg-HA nanocomposite beads were shown in Fig. 4. In general, the Coll-Alg-HA beads had a porous microstructure (Fig. 4a). Compared with Coll-Alg beads, a large amount of inorganic objects could be observed in the mineralized Coll-Alg fibrillar network, and the mineralization deposition led to the reduction of the pores. The magnified images (Fig. 4b, c, d) further revealed that inorganic nanoparticles were deposited mainly on the surfaces of the nanofibers. These SEM results confirmed that the Coll-Alg microgels with the Ca-capturing capability functioned as a 3D microreactor and were effective for developing Coll-Alg-HA nanocomposites. Energy dispersive X-ray (EDX) analysis was performed in a well-defined region of the mineralized nanofibrous matrix to examine the composition of the deposited inorganic phase, and its EDX trace was shown in Fig. 5. The presence of Ca and P peaks was evident and the average Ca/P ratio was 1.71, very close to that of stoichiometric hydroxyapatite (Ca/P = 1.67). A slight higher Ca/P ratio obtained in this study was probably due to the pre-incubation in calcium solution through both ionic interaction with negative charged groups and the physical entrapment as a result of the 3D network of the polymeric matrix.

3.2 Composition and structure confirmation

The FTIR spectra of Coll-Alg, Ca-captured Coll-Alg, and Coll-Alg-HA samples were presented in Fig. 6. The peptide bond vibrations of amide I, amide II and amide III of collagen are generally located at 1657, 1548, and 1244 cm^{-1}, respectively [13]; the characteristic peaks of alginate are at 1619 and 1420 cm^{-1} corresponding to the symmetrical and asymmetrical stretching modes of carboxyl group of alginate [6]. In the case of Coll-Alg samples (Fig. 6a), two strong peaks at 1631–1634 and 1480 cm^{-1} were recorded. Compared with the spectral features of pure collagen and alginate, the FTIR spectrum of Coll-Alg samples suggested the existence of molecular interactions between collagen and alginate molecules occurred in the preparation of Coll-Alg beads. After pre-incubation in the $CaCl_2$ aqueous solution, no extra band and obvious shift of any bands was observed in the FTIR spectrum of Ca-captured Coll-Alg samples (Fig. 6b). But, the relative intensity of the band at 1480 cm^{-1} decreased, probably relating to chelating calcium ions and active radicals such as carboxyl groups. It is worthy to notice that only slight differences in

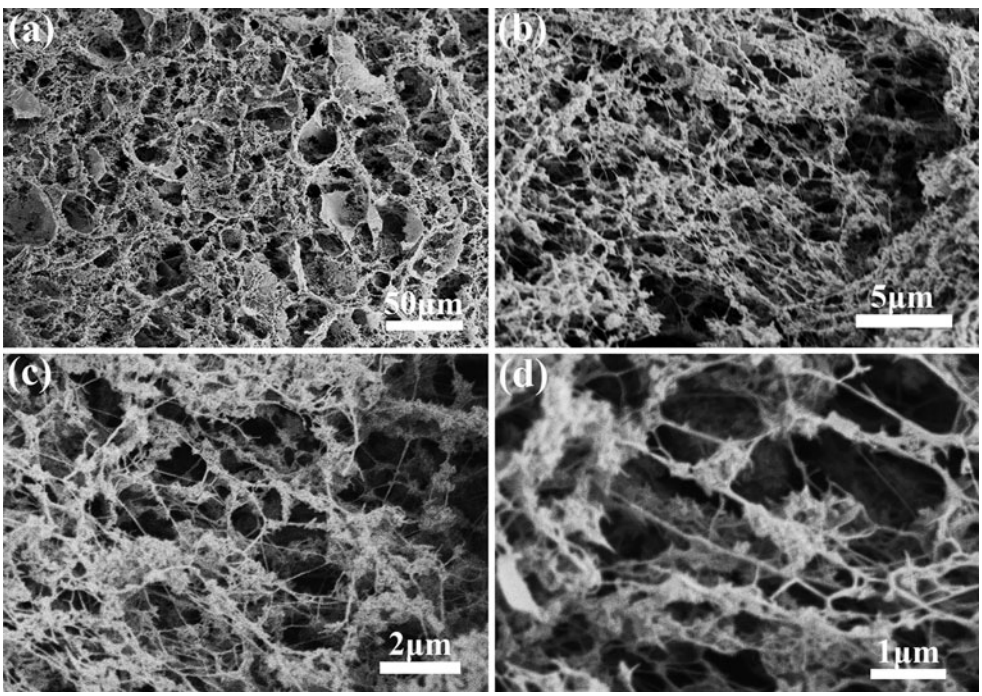

Fig. 4 Cross-sectional SEM images of the Coll-Alg-HA nanocomposite beads

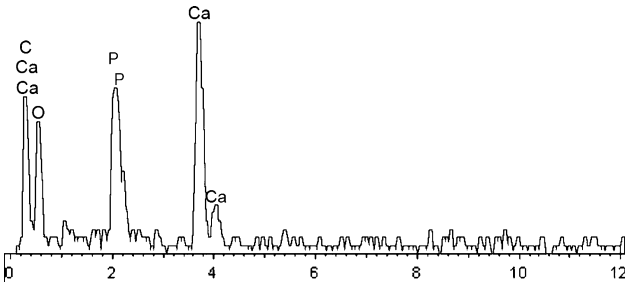

Fig. 5 Energy dispersive X-ray (EDX) trace of Coll-Alg-HA nanocomposite beads

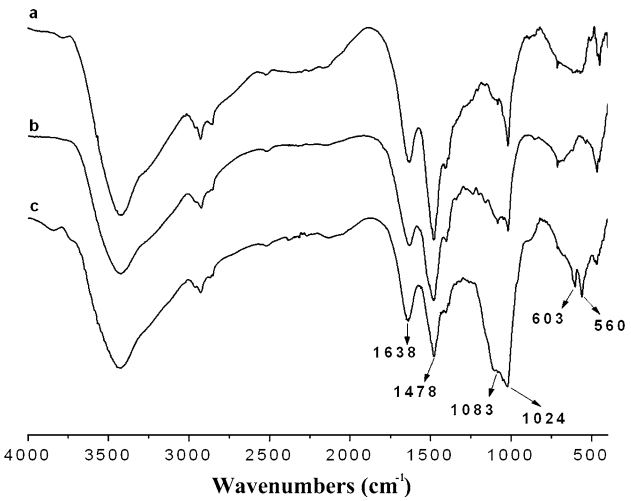

Fig. 6 FTIR spectra of (*a*) Coll-Alg matrices, (*b*) Ca-captured Coll-Alg matrices and (*c*) Coll-Alg-HA beads

the width or height of characteristic COO^- bands was also reported in terms of the chelating interaction between carboxyl group of alginate and calcium ions [2]. For the Coll-Alg-HA nanocomposites (Fig. 6c), the new adsorption peaks at 560, 603, 1022, and 1084 cm^{-1} were assigned to the stretching vibrations of phosphate groups of HA [11–13], confirming the formation of crystalline HA during the alternative mineralization of Coll-Alg microgels. In fact, the further reduction of the relative intensity of the adsorption at 1480 cm^{-1} supported the presence of chelating interactions between calcium ion and organic species [2].

Figure 7 showed the comparative XRD patterns of the Coll-Alg beads and Coll-Alg-HA nanocomposite beads. The broad peak centered at $2\theta = 22°$ was characteristic of Coll-Alg organic matrices (Fig. 7a). In the Coll-Alg-HA beads (Fig. 7b), this broad disappeared, and new reflections were recorded, attributable to HA [11, 24]. The strong reflections at 25.8° and centered at 32° (2θ), and minor reflections at 46.8, 49.4 and 53° corresponded to the (002), (211), (222), (312) and (213) plane of HA, respectively.

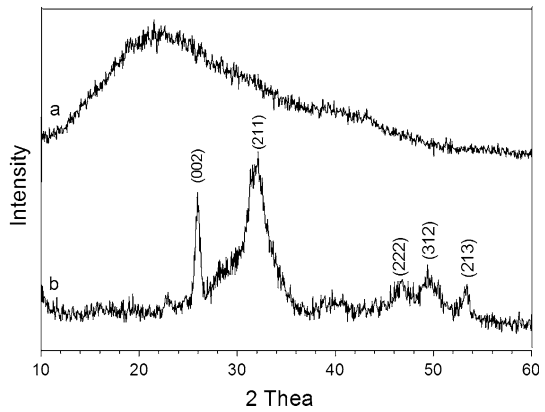

Fig. 7 XRD patterns of (*a*) Coll-Alg matrices and (*b*) Coll-Alg-HA nanocomposite beads

The broad nature of these reflections suggested that the synthetic HA of the nanocomposites was poorly crystalline bone-like apatite. The strong (002) reflection in relation to the intensity of (211) reflection indicated the occurrence of preferably orientated growth of apatite nanocrystals along organic fibers.

3.3 Deposition efficiency

The comparative TGA curves of Coll-Alg and Coll-Alg-HA beads were given in Fig. 8 to evaluate the deposition efficiency after three cycles of the alternative soaking process. In the case of the Coll-Alg organic matrices (Fig. 8a), the weight loss of 15.5 wt% occurred between 35 and 150°C, attributable to the liberation of the free water of the matrices and the decomposition of collagen helix structure. The significant weight loss of 64.5 wt% in the range of 230 ~ 500 °C was mainly a result of decomposition of collagen and alginate. Above 500°C, no further weight loss was recorded, and the total weight loss was 79 wt%, indicative of full carbonation in N_2 environment.

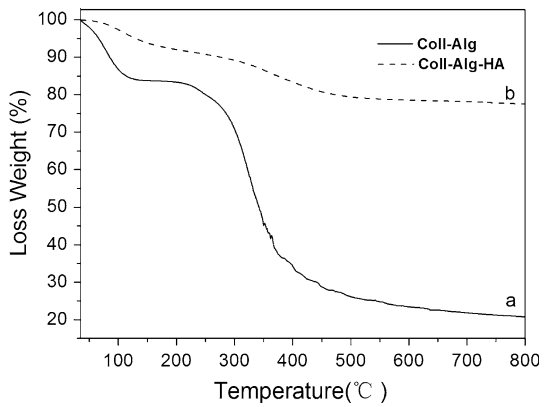

Fig. 8 TGA curves of (*a*) Coll-Alg matrices and (*b*) Coll-Alg-HA nanocomposite beads

In contrast, for the Coll-Alg-HA nanocomposites (Fig. 8b), there was a 23 wt% weight loss mainly over the whole range of 35–800°C, corresponding to the thermal decomposition of organic polymers. It is also notable that the decomposition peak of the organic substrate was delayed in the Coll-Alg-HA nanocomposite beads, which suggested that the integration of HA improved the thermal stability of the Coll-Alg matrices. The deposition efficiency of HA nanocrystals onto Coll-Alg matrices was achieved at 60.8 wt%, confirming that the present strategy is efficient.

Above all, the self-assembled Coll-Alg microgels, which functioned as a 3D microreactor, have been proved to be promising biomimetic matrices for the synthesis of bone-like nanocomposites. The salient features of the present strategy lie in: (1) the combination of collagen with alginate to enhance a highly porous architecture for ease infiltration of inorganic ions [23], (2) additionally providing anionic functional groups (ie. carboxyl group) to endow the Ca^{2+} capturing capability of the self-assembled biomimetric matrices, thus securing the effective precipitation of HA nanocrystals. Meanwhile, the HA nanocrystals loaded onto the nanostructured microgels also reduced the mobility of the polymeric segments and further stabilized the three-dimensional network. These synergistic effects were believed to be responsible for the good spherical shape maintenance and less contraction of Coll-Alg-HA beads in contrast to the Coll-Alg composite beads. Moreover, the HA nanocrystals deposited on the fibrillar matrices also endowed the nanocomposites with extraordinary properties such as high surface area for loading bioactive factors and a cell-friendly surface bonding, potentially in drug delivery and cells ingrowth applications.

4 Conclusions

The present work reported a novel self-assembled protein-based matrix to synthesize polymer-HA nanocomposites. This porous architecture largely mimicked the natural extracellular matrix with a highly interconnected porous structure, appropriate for bone tissue regeneration. The integration of alginate directly endowed the biomimetic matrices with the Ca-capturing capability, which functioned as a 3D microreactor for subsequent deposition of HA via an alternative soaking process. The proposed methodology is efficient in the development of bone-like nanocomposites (beads).

Acknowledgements This work is supported by the National Natural Science Foundation of China (No. 30670561, 30970729 and 50830105), the Foundation of the Ministry of Education of China (No. 20090181110067) and the National Basic Research Program of China (No. 2005CB623903 and 2007CB936102). The support from DfES of the UK/China Fellowships for Excellence Programme is gratefully acknowledged.

References

1. Li JJ, Chen YP, Yin YJ, Yao FL, Yao KD. Modulation of nano-hydroxyapatite size via formation on chitosan-gelatin network film in situ. Biomaterials. 2008;28:781–90.
2. Ribeiro CC, Barrias CC, Barbosa MA. Calcium phosphate-alginate microspheres as enzyme delivery matrices. Biomaterials. 2004;24:4363–73.
3. Schachschal S, Pich A, Adler HJ. Aqueous microgels for the growth of hydroxyapatite nanocrystals. Langmuir. 2008;24:5129–34.
4. Zhao KY, Cheng GX, Huang JJ, Ying XG. Rebinding and recognition properties of protein-macromolecularly imprinted calcium phosphate/alginate hybrid polymer microspheres. React Func Polym. 2008;68:732–41.
5. Jongpaiboonkit L, Franklin-Ford T, Murphy WL. Mineral-coated polymer microspheres for controlled protein binding and release. Adv Mater. 2009;21:1–4.
6. Zhang J, Wang Q, Wang A. In situ generation of sodium alginate/hydroxyapatite nanocomposite beads as drug-controlled release matrices. Acta Biomateria. 2010;6:445–54.
7. Góes JC, Figueiró SD, Oliveira AM, Macedo AAM, Silva CC, Ricardo NMPS, Sombra ASB. Apatite coating on anionic and native collagen films by an alternate process. Acta Biomateria. 2007;3:773–8.
8. Kawashita M, Nakao M, Minoda M, Kim HM, Beppu T, Miyamoto T, et al. Apatite-forming ability of carboxyl group-containing polymer gels in a simulated body fluid. Biomaterials. 2003;24:2477–84.
9. Miyazaki T, ohtsuki C, Akioka Y, Tanihara M, Nakao J, Sakaguchi Y, et al. Apatite deposition on polyamide films containing carboxyl group in a biomimetic solution. J Mater Sci Mater Med. 2003;14:569–74.
10. Jen T, Huang HH, Lan CW, Lin CH, Hsu FY, Wang YJ. Studies on the microspheres comprised of reconstituted collagen and hydroxyapatite. Biomaterials. 2004;25:651–8.
11. Wang XM, Wang XL, Ma JF, Zheng GQ, Chen ZH, Li XD. Versatile nanostructured processing strategy for bone grafting nanocomposites based on collagen fibrillogenesis. Adv Appl Ceram. 2009;108:384–8.
12. Li X, Chang J. Preparation of bone-like apatite-collagen nanocomposites by a biomimetic process with phophorylated collagen. J Biomed Mater Res A. 2008;85:293–300.
13. Wang XL, Wang XM, Tan YF, Zhang B, Gu ZW, Li XD. Synthesis and evaluation of collagen-chitosan-hydroxyapatite nanocomposites for bone grafting. J Biomed Mater Res A. 2009;89:1079–87.
14. Beekman B, Verzijl N, Ban RA, Von der Mark K, TeKoppele JM. Synthesis of collagen by bovine chondrocytes cultured in alginate: posttranslational modifications and cell-matrix interaction. Exp Cell Res. 1997;237:135–41.
15. Choi YS, Hong SR, Lee YM, Song KW. Study on gelatin-containing artificial skin: I. preparation and characteristics of novel gelatin-alginate sponge. Biomaterials. 1999;20:409–17.
16. Dvir-Ginzberg M, Gamlieli-Bonshtein I, Agbaria R, Cohen S. Liver tissue engineering within alginate scaffolds: effects of cell-seeding density on hepatocyte viability, morphology, and function. Tissue Eng. 2003;9:757–66.
17. Grant GT, Morris ER, Rees DA, Smith PJC, Thom D. Biological interactions between polysaccharides and dicalent cations: the egg box model. FEBS Lett. 1973;32:195–8.

18. Eiselt P, Julia Y, Latvala RK, Shea LD, Mooney DJ. Porous carriers for biomedical applications based on alginate hydrogels. Biomaterials. 2000;21:1921–7.
19. Tsai SW, Hus FY, Chen PL. Beads of collage-nanohydroxyapatite composites prepared by a biomimetic process and the effects of their surface texture on cellular behavior in MG 63 osteoblast-like cells. Acta Biomateria. 2008;4:1332–41.
20. Suzuki K, Yumura T, Mizuguchi M, Taguchi T, Sato K, Tanaka J, Akashi M. Apatite-silica gel composite materials prepared by a new alternate soaking process. J Sol Gel Sci Technol. 2001;21:55–63.
21. Furuzono T, Taguchi T, Kishida A, Akashi M, Tamada Y. Preparation and characterization of apatite deposited on silk fabric using an alternate soaking process. J Biomed Mater Res. 2000;50:344–52.
22. Hui TY, Cheung KMC, Cheung WL, Chan D, Chan BP. In vitro chondrogenic differentiation of human mesenchymal stem cells in collagen microspheres: influence of cell seeding density and collagen concentration. Biomaterials. 2008;29:3201–12.
23. Grande CJ, Torres FG, Gomez CM, Bañó MC. Nanocomposites of bacterial cellulose/hydroxyapatite for biomedical applications. Acta Biomateria. 2009;5:1605–15.
24. Koutsopoulos S. Synthesis and characterization of hydroxyapatite crystals: a review study on the analytical methods. J Biomed Mater Res. 2002;62:600–12.